Laser and Particle Beams (2001), *19*, 647–655. Printed in the USA.

DOI: 10.1017.S0263034601194127

CO_2 laser ion source: Comparison between mode-locked and free-running laser beams

N. LISI,[1,2] C. MEYER,[1] AND R. SCRIVENS[1]
[1]CERN PS Division, CH-1211 Geneve 23, Switzerland

(RECEIVED 2 April 2001; ACCEPTED 27 June 2001)

Abstract

The production of highly charged ions in a CO_2 laser-generated plasma is compared for different laser pulse-time structures. The work was performed at the CERN Laser Ion Source, which has the aim of developing a high current, high charge-state ion source for the Large Hadron Collider (LHC). When an intense laser pulse is focused onto a high-*Z* metal target, the ions expanding in the plasma plume are suitable for extraction from the plasma and matching into a synchrotron. For the first time, a comparison is made between free-running pulses with randomly fluctuating intensity, and mode-locked pulse trains with a reproducible structure and the same energy. Despite the lower power density with respect to the mode-locked pulse train, the free-running pulse provides higher charge states and higher yield.

Keywords: Heavy ions; Ion sources; Laser; Plasma

1. INTRODUCTION

At the CERN Laser Ion Source (LIS), studies are made of ion generation and extraction from laser-produced plasmas, and the injection of this ion current pulse into a linear accelerator (Haseroth *et al.*, 1998; Sharkov *et al.*, 1998; Fournier *et al.*, 2000). The aim is to produce a 5-μs pulse of highly charged lead or tantalum ions (Pb^{25+}, Ta^{25+}) containing at least 10^{10} particles that would allow single turn injection into the Proton Synchrotron Booster (PSB). The ion pulse should have a high shot-to-shot reproducibility and low beam noise during the injection period. The present layout of the LIS is shown in Figure 1. Most of the measurements are performed with tantalum targets mainly for its isotopic purity and high melting point (which reduces target damage and sputtering onto optical components). To satisfy the specified parameters, an upgraded laser system consisting of a Master Oscillator (MO; Haseroth *et al.*, 1998) and a new power amplifier able to deliver 100-J, 20-ns laser pulses at a repetition rate of 1 Hz ($\lambda = 10.6$ μm) is being constructed (Makarov *et al.*, 2001).

The present study was performed in order to define the time structure of the seed pulse that will be fed into the power amplifier. The performance of the CERN LIS with single-mode and free-running (FR) laser pulses was studied in the past (Scrivens, 1999) and little difference was found in the ion yields. Single-mode laser pulses are advantageous, as optical elements are further from the damage threshold and the pulses are more reproducible.

The power density of the laser is an important scaling parameter (Baranov, 1996) as shown in Figure 2. A pulse-train mode-locked (ML) laser pulse will increase the power density on the target surface for the same laser energy. The pulse-train mode could then be expected to enhance the charge state produced, thus allowing a lower total laser energy. A statistical stabilizing effect due to the presence of several short pulses can be expected, as the ion generation process would be split into several successive processes rather than a single one. Submillimeter diameter uniform plasmas with the observed ion velocity (from 4×10^5 to 4×10^4 ms^{-1}) will expand in vacuum in a few nanoseconds. A pulse-train spacing of the order of 10 ns therefore allows considerable expansion of the plasma between pulses.

2. THE CERN LASER

The new laser system under construction should provide sufficient ions in the correct charge state. Meanwhile the ion extraction and the beam transport are being studied using a lower energy laser (Lumonics TEA600). Such a laser system provides nearly the desired number of particles at a lower charge state (Ta^{20+}). When the TEA600 laser is used

Address correspondence and reprint requests to: Nicola Lisi, ENEA Casaccia, P.O. Box 2400, 00100 Rome, Italy. E-mail: nicola.lisi@casaccia.enea.it
[2]Present address: ENEA Casaccia, PO Box 2400, 00100 Roma, Italy

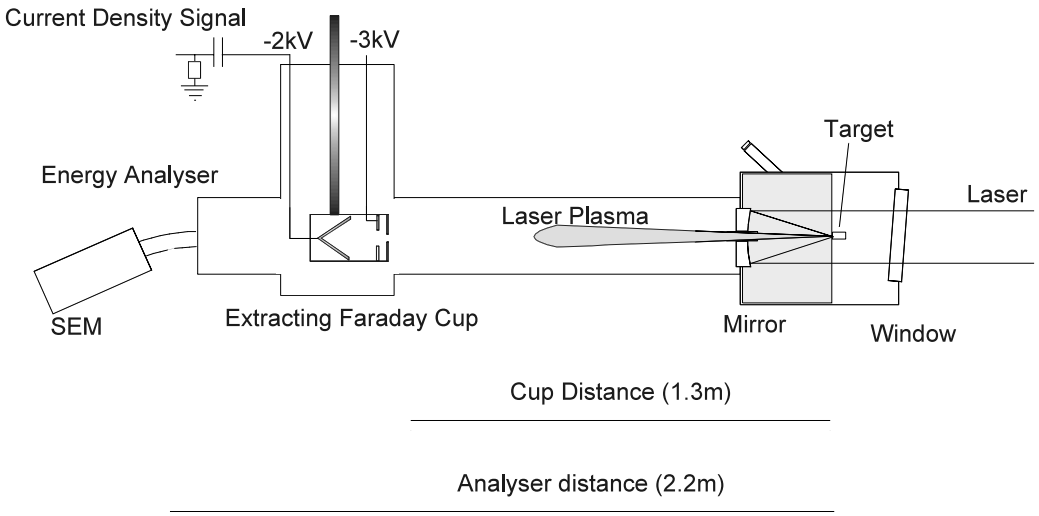

Fig. 1. Scheme of the LIS source. Keeping the positive and the negative electrode at ground potential allows the plasma to drift undisturbed to the extracting Faraday cup. An electrostatic analyzer with a secondary emission multiplier (SEM) detector measures the charge-state distribution.

as a free-running oscillator equipped with an unstable resonator, it is able to deliver 30 J of energy (20 J in the first 100 ns spike) and the power density on target is measured to be 2.0×10^{12} W/cm^2. The copper parabolic focusing mirror has a focal length of 0.3 m. It has a central aperture that allows the plasma plume to drift towards the extraction area. The laser beam diameter on the copper mirror is 12 cm. As an alternative to the TEA600 free-running unstable resonator, an amplifier chain was set up at CERN. The MO generates the seed pulse. A second laser system, Lumonics TEA103/3, was installed and converted into a single-pass preamplifier, while the TEA600 was modified to be a three-pass power amplifier.

3. MODE-LOCKED MASTER OSCILLATOR

The MO consists of a transverse electric discharge module at atmospheric pressure (TEA) and a low-pressure tube (LPT) that narrows the spectral gain and makes possible single longitudinal mode operations. The LPT can be removed to deliver a free-running, randomly spiked pulse. When an acousto-optic modulator (AOM; NEOS N12041-6-WC) is inserted in the cavity (Fig. 3) and driven at an RF frequency synchronous with the cavity round trip, the MO is mode locked and delivers a reproducible train of short pulses. The rise time of each pulse was measured to be in the range of 1 ns. By reducing the RF power in the modulator, the MO

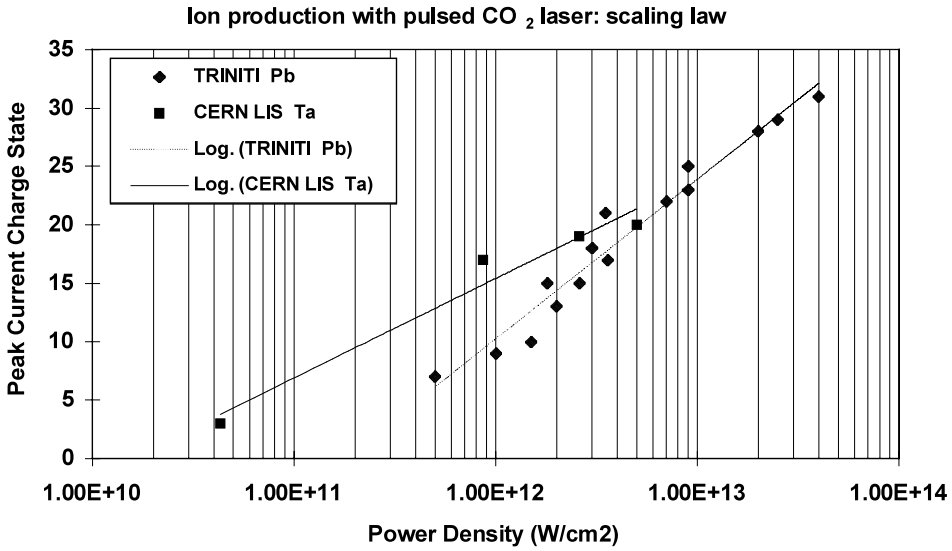

Fig. 2. Scaling law for CO_2 laser ion generation. The charge state carrying most of the current versus "vacuum" power density on target.

https://doi.org/10.1017/S0263034601194127 Published online by Cambridge University Press

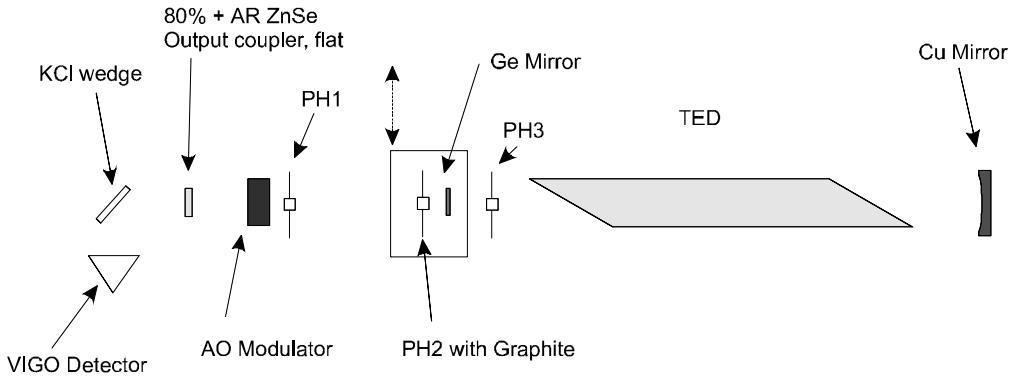

Fig. 3. Scheme of the mode-locked Master Oscillator.

delivers a free-running pulse, with the random intensity fluctuations typical of TEA CO_2 lasers. The AOM is made of a germanium crystal with antireflection (AR) coatings on both surfaces and a piezo-electric transducer driven by an RF signal. The losses for one polarization are 30% when a power of 7 W is fed into the cavity. The correct polarization is selected in the laser cavity by means of the two Brewster angle salt (NaCl) windows of the TEA module.

The RF signal is first produced by a frequency generator (41.07 MHz), amplified, and fed into the AOM. The correct RF power is selected by adjusting a variable attenuator between the signal generator and the RF amplifier. The generator frequency is matched manually to the crystal resonance by monitoring and minimizing the reflected RF signal. Since the crystal was not kept in an oven, the resonant frequency shifted during the experiment due to temperature drifts, but for a few hours, stable operation could be achieved. The active aperture of the AOM (PH1 in Fig. 3) is 6 mm, which provides single transverse mode operation of the MO (TEM00).

The output coupler of the cavity was a ZnSe flat mirror with 80% reflection on one of the surfaces and with an AR coating on the other. The scheme of the MO is shown in Figure 3. Also a 30% output coupler mirror was tested, but the quality of the resonator was not sufficient to observe mode locking. The reason was some damage on the AR coatings of the modulator due to the excessive laser energy density. The damage on the AR coatings increases the round trip losses, making necessary the use of the 80% reflectivity output coupler.

4. MASTER OSCILLATOR ALIGNMENT AND OPERATION

The alignment of the laser system was problematic due to the wedge angle of the Modulator (30′) and its small aperture (PH1 = 6 mm), and was achieved by building a two-stage cavity. The final optical alignment of the laser was performed by optimizing the near-field pattern of the laser beam onto a graphite screen and then the beam energy. A laser pulse energy of less than 10 mJ measured both for FR and ML operation, compared to 100 mJ when the AOM was not inserted in the cavity and a 30% reflecting output coupler was used. The lower energy was mainly due to the high losses from the AOM surfaces after some damage to the AR coatings. In principle, the use of a modulator at the Brewster angle could allow much higher energy density on the surface before damage occurs, but it would require four times as much RF power. In Figure 4, the pulse shapes of the typical free-running and mode-locked pulses, when an RF power of 5 W was fed into the AOM, are reported. The pulses are measured with a fast photoelectromagnetic detector (VIGO Systems PEM-L-3).

5. AMPLIFIER CHAIN

A sketch of the amplifier optical scheme is shown in Figure 5. The laser pulse from the MO passes through a telescope consisting of two spherical mirrors with 2-m and 4-m radius that doubles the beam size. A 1-mm aperture in the confocal position of the telescope acts as a spatial filter and reduces the parasitic back-reflection from the plasma, protecting the MO output coupler. The spatial filter consists of a 1-mm-diameter hole in an aluminum blade in air. After the first telescope, the beam is amplified by the single-pass laser preamplifier (Lumonics TEA 103) and then in the three-pass amplifier (Lumonics TEA600). Both amplifiers are equipped with Brewster angle windows. The three-pass amplification is achieved by means of a telescope equipped with a 4.4-m radius convex mirror and a 34-mm-diameter, 1.4-m-radius concave mirror. After amplification, the laser beam has a diameter of $\sim$8 cm and is transported to the target via five flat copper mirrors across a 30-m-long path. The beam energy measured with a pyroelectric joule-meter was 7 mJ and 6 mJ from the master oscillator for FR and ML respectively, and 300 mJ and 280 mJ with preamplification. The energy measured in front of the target chamber using a calorimeter was 8 ± 1 J both for FR and ML operation. The laser waveform was measured in front of the target chamber by observing the radiation scattered from the surface of the last copper mirror with the VIGO detector. Two typical waveforms for mode-locked and free-running operation are presented in

https://doi.org/10.1017/S0263034601194127 Published online by Cambridge University Press

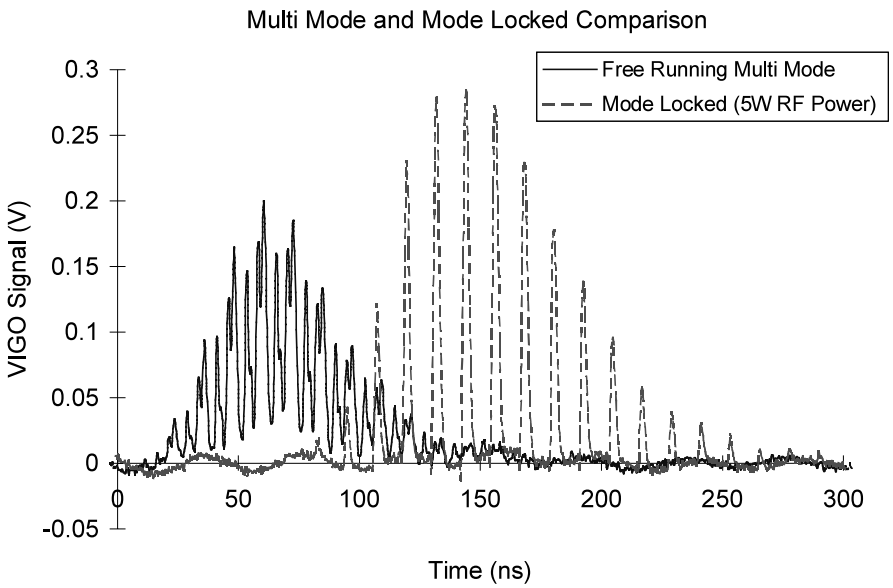

Fig. 4. Comparison of free-running and mode-locked pulses from the Master Oscillator. The FR pulse energy is 7 mJ, while the ML pulse energy is 6 mJ.

Figure 6. The focused beam was measured to be nearly diffraction limited (Scrivens, 1999) for a 100-μm spot. Thus an estimate of the power density is 1.5×10^{12} W/cm^2 and 3×10^{12} W/cm^2 for the free-running and mode-locked pulses, respectively. The duration of both the free-running pulse and the mode-locked pulse train is around 70 ns.

6. PLASMA CURRENT DENSITY

The plasma current is measured with an extracting Faraday cup placed some distance from the target. By biasing the collector electrode at -2 kV and the suppression ring at -3 kV, an accurate measurement of the total plasma current entering the cup can be obtained. By knowing the aperture of the cup (d_{cup} = 6.5 mm) and the cup-to-target distance (l_{cup} = 1.3 m), the current density at a distance of 1 m can be obtained, since the current density of the expanding plasma decreases with the inverse cube of the distance (due to the spherical geometric expansion and to the initial velocity spread). In Figure 7, the ion current waveform is shown, averaged over 10 laser shots. Except for a small peak arriving in the first 2 μs (due to lighter ions from surface contamination of the target), the ions generated with the mode-locked laser beam are slower. The small current peak of fast

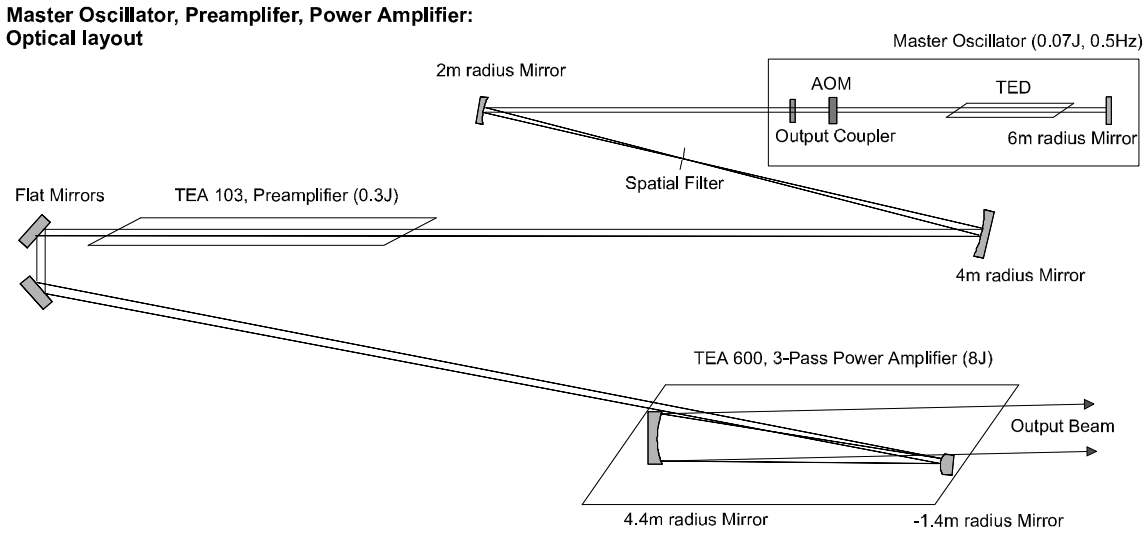

Fig. 5. Scheme of the amplification chain.

https://doi.org/10.1017/S0263034601194127 Published online by Cambridge University Press

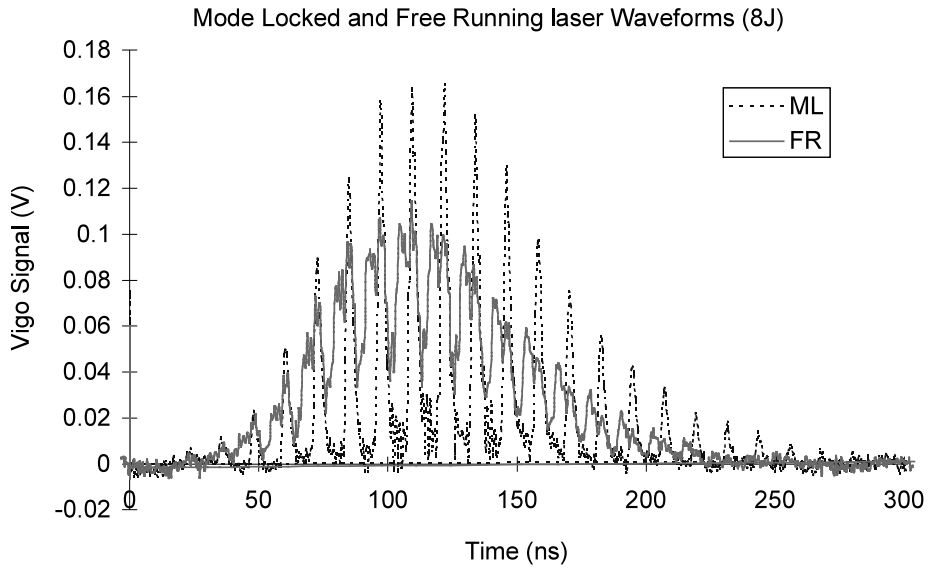

Fig. 6. Comparison of two typical mode-locked and free-running pulses in front of the target chamber.

ions arriving in the first 2 μs was due to some hydrocarbon contamination of the target surface.

7. CHARGE STATE DISTRIBUTIONS

After removing the Faraday cup, the charge state distribution (CSD) was measured. The CSD is measured by varying the voltage across the two parallel plates of the energy analyzer and recording the traces obtained for each voltage. For each value of the field, a time-of-flight spectrum similar to that shown in Figure 8 was obtained.

By measuring the arrival time and the intensity of each different charge state and by taking into account the target-to-spectrometer distance, the charge state distributions, given in Figures 9 and 10, for the free-running and mode-locked pulse train mode were obtained. Despite the higher power density of the mode-locked pulse train, the ions are slower and the average charge state is lower.

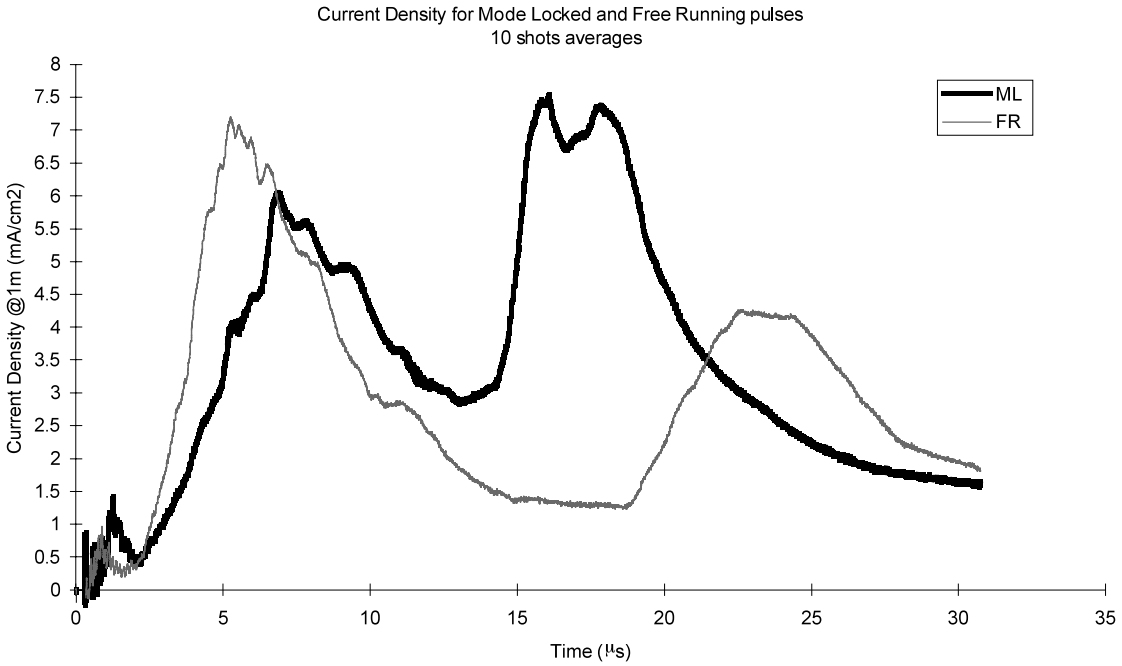

Fig. 7. Current density waveform for mode-locked and free-running laser beams. The first current peak (3–8 μs) contains the highly charged ions.

https://doi.org/10.1017/S0263034601194127 Published online by Cambridge University Press

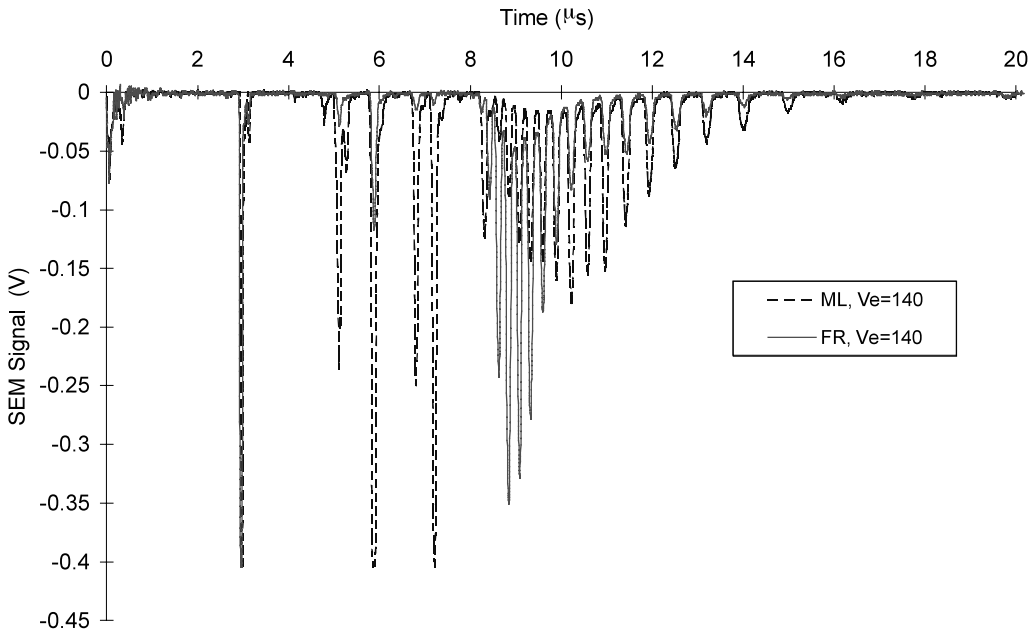

Fig. 8. Recorded time of flight spectra for mode-locked and free-running pulses. The analyzer voltage is 140 V. The analyzer is 2.2 m from the target.

The highly charged ions arrive between 3 and 8 μs after the laser pulse. The second structure in the current waveform, seen in Figure 6 at later times (after 15 μs), is due to ions with lower charge.

8. DISCUSSION

In this paper, a free-running laser pulse and a mode-locked pulse train are amplified to equal energy and are compared with respect to ion generation in the laser–plasma interaction. Despite the higher power density of the mode-locked case, the free-running pulse seems more effective in generating and accelerating highly charged ions in the plasma. A consequence of these results is that the power density on target is not the only relevant scaling parameter for the ion generation and ion acceleration processes. Since the charge state distribution in a CO_2 laser plasma's expanding plume is not dominated by recombination (Roudskoy, 1996), an explanation is that, during the shorter laser pulse (5 ns), there is not enough time for the collisional heating of the

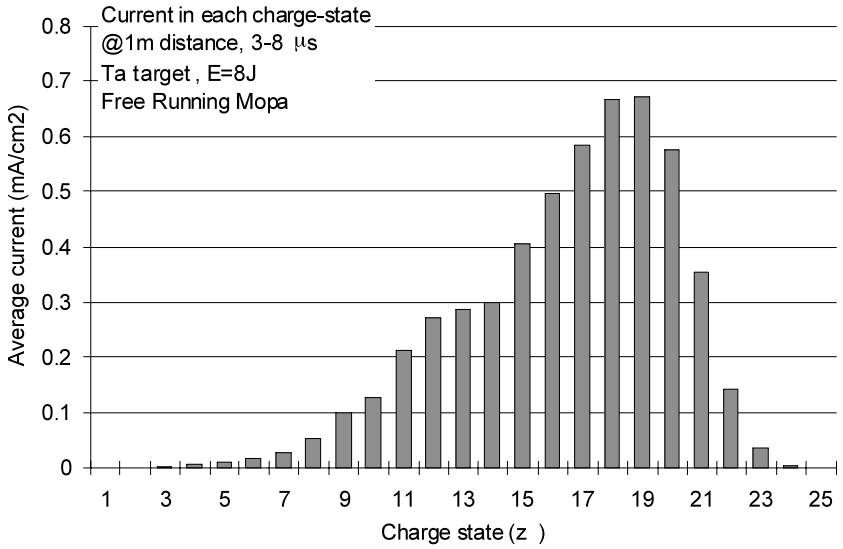

Fig. 9. Charge-state distribution with free-running pulse.

https://doi.org/10.1017/S0263034601194127 Published online by Cambridge University Press

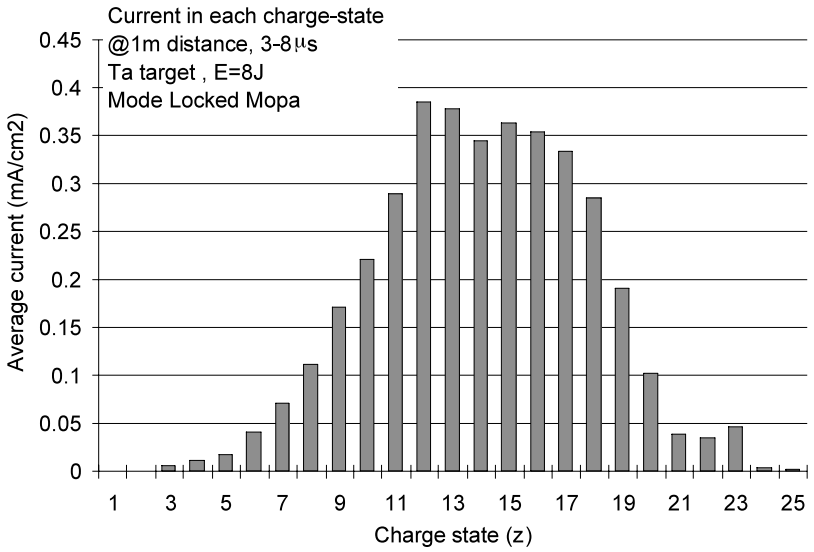

Fig. 10. Charge-state distribution with mode-locked pulse train.

ions to reach a stationary state, and a lower charge state is thus observed.

The electron temperature in the plasma rapidly decreases in the "dark" time period between subsequent pulses, effectively stopping the ionization process of the higher charge states. The rapid decrease of the electron temperature is due to plasma expansion, electron heat conduction, and radiation.

If we consider the simplest geometry of a spherical plasma with a diameter of 200 μm and a particle velocity of the order of 5×10^5 m/s, the plasma will double its size in only 1 ns. In the case of an adiabatic expansion, thus neglecting other temperature decrease mechanisms such as radiation and heat conductivity to the colder plasma regions, the temperature will decrease to half its initial value in 1 ns.

The equilibrium charge state distributions were calculated following Colombant and Tonon (1973), and by fitting the high charge end of the charge state distributions measured with the free-running laser, the electron temperature was estimated to be around 150 eV. This is the temperature of the plasma where the stepwise collisional ionization and recombination processes take place. Subsequent recombination should not substantially alter the populations of highly charged ions (Colombant & Tonon, 1973; Roudskoy, 1996) during the plasma expansion.

The time necessary for stepwise ionization of Ta at critical electron density ($n_e = 10^{19}$ cm^{-3}) was calculated as a function of charge state and electron temperature by neglecting recombination (Colombant & Tonon, 1973). The time required for the production of the ion with charge z via stepwise ionization can be calculated from the ionization rates using the following expression:

$$\tau_z \approx \frac{1}{n_e} \sum_{1}^{z} \frac{1}{S(i-1, T_e)} \tag{1}$$

Here z is the charge, S is the ionization rate (cm^{3}s^{-1}) and is a function of the electron temperature T_e, and n_e is the electron density (cm^{-3}). Several similar expressions for the electron impact ionization rate are available in the literature. The time to reach a stationary population of charge state Ta^{20+} has been calculated as a function of the electron temperature using three different expressions of the ionization coefficient (S) available in literature: Eq. (2) (Mima, 1994); Eq. (3) (Colombant & Tonon, 1973); and Eq. (4) (McWhirter, 1965):

$$S_1(z, T_e) = 2.15 \cdot 10^{-6} \xi_z T_e^{1/2} e^{-(E_z/T_e)} \frac{1}{E_z^2} \text{ (cm}^3\text{/s)} \tag{2}$$

$$S_2(z, T_e) = \frac{9 \cdot 10^{-6} \xi_z (T_e/E_z)^{1/2}}{E_z^{3/2}(4.88 + T_e/E_z)} e^{-(E_z/T_e)} \text{ (cm}^3\text{/s)} \tag{3}$$

$$S_3(z, T_e) = 2.43 \cdot 10^{-6} \xi_z T_e^{-3/2} e^{-(E_z/T_e)} \frac{1}{(E_z/T_e)^{7/4}} \text{ (cm}^3\text{/s)} \tag{4}$$

Here T_e is the electron temperature (in electron volts) while E_z is the ionization energy of an ion of charge z (in electron volts) and ξ_z is the number of electrons in the outer shell of the ion of charge z, that are likely to be excited by low energy electron impact. In Figure 11, it can be seen that there is a basic agreement between the three expressions.

Using Eq. (3) it is seen in Figure 12 that 50 ns are required to produce Ta^{20+} when the electron temperature is approximately 150 eV. When the electron temperature is increased, the ion heating stage becomes shorter and the laser pulse length required for a given charge state can be reduced. In our experiment with shorter pulses, a sufficient electron temperature for effective production of the high charge states was not reached. The temperature of the plasma should be at

https://doi.org/10.1017/S0263034601194127 Published online by Cambridge University Press

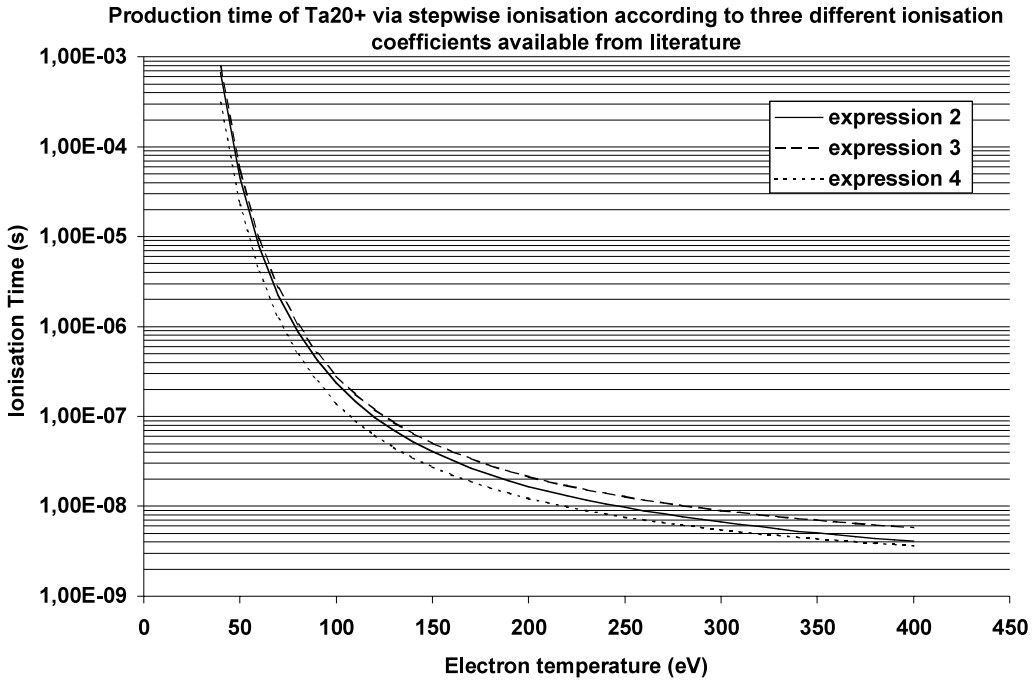

Fig. 11. Time required for reaching an equilibrium population of Ta $^{20+}$ according to expression (1) for three different ionization coefficient expressions.

least 350 eV for the efficient production of Ta^{20+} in a time as short as 5 ns. For a more precise estimation of the ionization time, recombination processes should be taken into account, but at the CO_2 laser wavelength's critical electron density of 10^{19} cm^{-3}, their contribution was neglected.

9. CONCLUSIONS

For the first time, the ion production yield using a mode-locked train of short laser pulses was measured and a comparison was made with a free-running laser pulse of the

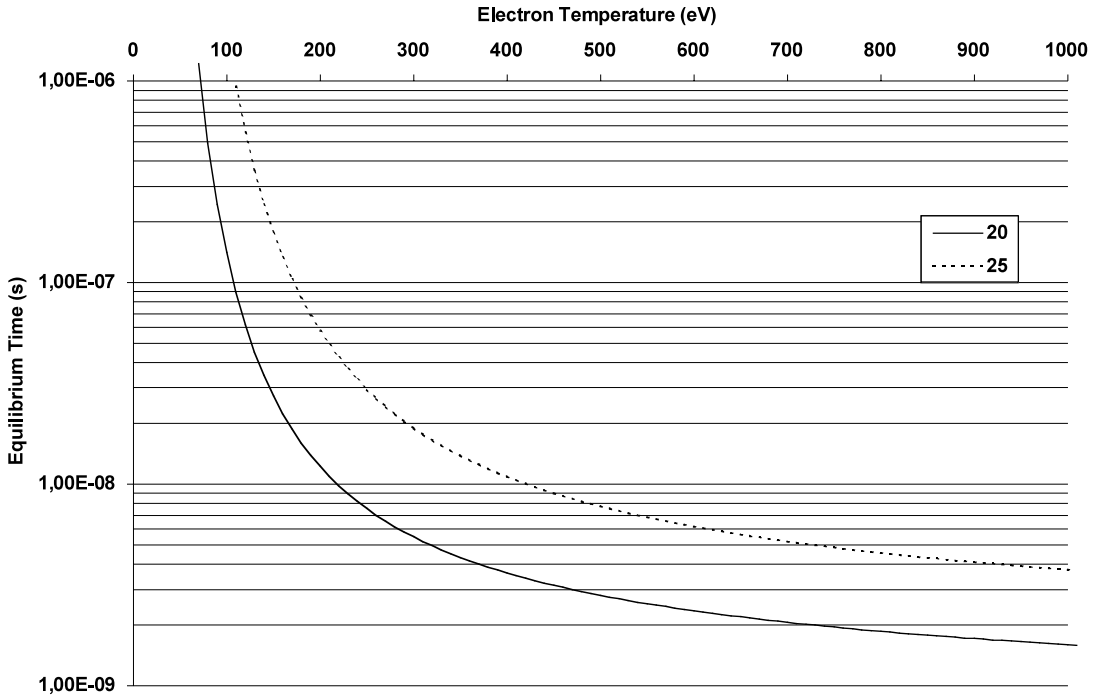

Fig. 12. Excitation time of a given charge state as a function of electron temperature ($n_e = 10^{19}$ cm^{-3}).

https://doi.org/10.1017/S0263034601194127 Published online by Cambridge University Press

same average intensity on target. This mode of operation did not improve the situation with respect to a free-running pulse with the same energy and the same duration. This can be explained by an insufficient time for achieving the equilibrium charge-state distribution inside the CO_2 laser-produced plasma. Pulse-train operation could be advantageous for shorter laser wavelength where the higher plasma density shortens the ionization time.

REFERENCES

Baranov, V.Yu., Makarov, K.N., Roerich, V.C., Satov, Yu.A., Starostin, A.N., Stepanov, A.E., Sharkov, B.Yu., Langbein, K. & Sherwood, T.R. (1996). Study of multicharged heavy ion generation from CO_2 laser-produced plasma. *Laser Part. Beams* **14**, 347–369.

Colombant, D. & Tonon, G.F. (1973). X-ray emission in laser-produced plasmas. *J. Appl. Phys.* **44**, 3524–3537.

Fournier, P., Gregoire, G., Kugler, H., Haseroth, H., Lisi, N., Meyer, C., Ostroumov, P., Schnuriger, J.C., Scrivens, R., Rodriguez, F.V., Wolf, B.H., Homenko, S., Makarov, K., Satov, Y., Stepanov, A., Kondrashev, S., Sharkov, B. & Shumshurov, A. (2000). Status of the CO_2 laser ion source at CERN. *Rev. Sci. Instrum.* **71**, 924–926.

Haseroth, H., Kugler, H., Langbein, K., Lisi, N., Lombardi, A., Magnusson, H., Pirkl, W., Schnuriger, J.C., Scrivens, R., Tambini, J., Tankle, E., Homenko, S., Makarov, K., Roerich, V., Stepanov, A., Satov, Y., Kondrashev, S., Savin, S., Sharkov, B., Shushurov, A., Krása, J., Láska, L., Pfeifer, M. & Woryna, E. (1998). Developments at the CERN laser ion source. *Rev. Sci. Instrum.* **69**, 1051–1053.

Makarov, K.N., Malyuta, D.D., Nishchuk, S.G., Roerich V.C., Satov, Yu.A., Smakovskii, Yu.B., Stepanov, A.E. & Khomenko, S.V. (2001). Study of the dynamics of propagation of CO_2 laser pulses in a chain of non-linear absorbing and amplifying media. *Quant. Electron.* **31**, 23–29.

McWhirter, R.W.P. (1965). In *Plasma Diagnostic Techniques* (Huddelstone, R.H., and Leonard, S.I., Eds.) p. 210. New York: Academic.

Mima, K., Baldis, H.A., Nishiguchi, A., Takabe, H. & Yamanaka, C. (1994). *Laser Plasma Theory and Simulation*. New York: Harwood Academic Publisher.

Roudskoy, I.V. (1996). General features of highly charged ion generation in laser-produced plasma. *Laser Part. Beams* **14**, 369–384.

Scrivens, R. (1999). *Extraction of an Ion Beam from a Laser Ion Source*. Ph.D. Thesis, CERN and University of Wales Swansea.

Sharkov, B.Y., Kondrashev, S., Roudskoy, I., Savin, S., Shumshurov, A., Haseroth, H., Kugler, H., Langbein, K., Lisi, N., Lombardi, A., Magnusson, H., Pirkl, W., Schnuriger, J.C., Scrivens, R., Tambini, A., Tanke, E., Homenko, S., Makarov, K., Roerich, V., Stepanov, A. & Satov, Y. (1998). Laser ion source for heavy ion synchrotrons. *Rev. Sci. Instrum.* **69**, 1035–1039.

https://doi.org/10.1017/S0263034601194127 Published online by Cambridge University Press